Proceedings of the 1998 IEEE/RSJ
Intl. Conference on Intelligent Robots and Systems
Victoria, B.C., Canada • October 1998

A Model-Based Impedance Control Scheme for High-Performance Hydraulic Joints

Glen Bilodeau[1] and Evangelos Papadopoulos[1,2]

[1]Dept. of Mechanical Engineering & CIM, McGill University, Montreal, PQ, Canada H3A 2A7
[2]Dept. of Mechanical Engineering, National Technical University of Athens, 15773 Zografou, Greece

Abstract

Impedance control of a hydraulic servoactuator joint system is discussed in this paper. Impedance control imparts a desired behavior to a system, rather than it controls position or force individually. Due to nonlinear properties of hydraulic actuators, impedance control is difficult. The control strategy presented here involves a combined feedforward and feedback control. An impedance filter modifies a desired trajectory according to a specified behavior. The modified trajectory is fed to a reduced-order model of the servoactuator hydraulic joint in order to reduce the effects of the nonlinear hydraulic dynamics. Position, velocity and pressure feedback loops compensate for the unmodeled dynamics. Simulation results show the strategy to be promising in providing impedance control to the joint. Special attention is given to the careful choice of impedance and control parameters to ensure smooth transition between contact and non-contact regimes, and to avoid actuator saturation. The developed controller is useful in achieving a desired behavior of hydraulic manipulators in contact tasks. It will provide the basis for a robust impedance control of the SARCOS high-performance hydraulic manipulator.

1 Introduction

Hydraulically actuated manipulators are increasingly important for a number of proposed applications. These include hazardous waste management, fire-fighting, and live-line maintenance. In mining and forestry industry, existing machinery is predominantly hydraulic and efforts are being made to automate or teleoperate such machines, for example, [12]. In all these applications, the manipulators are required to perform tasks in free space and have extensive interaction with objects or some environment. At least three factors complicate the automation/teleoperation of these tasks: (1) environment properties, (2) task requirements, and (3) manipulator characteristics. The environment may be stationary or moving, rigid or flexible. As an example, in live-line maintenance, the supporting poles may oscillate due to winds and swaying wires. In fire-fighting, the task of ventilation involves cutting a hole of at least one by one meter in the roof of a residence. Damage due to heat and contaminants severely influence a roof's properties. Next, a task may require the application of large forces. Reaction forces due to the tools used will also affect the progress of the task. Finally, manipulator characteristics like link, sensor and hydraulic actuator dynamics affect the joint control of the manipulator during tasks. Thus, from the applications and their requirements standpoint, there is a need to provide stable and robust force control of hydraulically actuated manipulators.

Hydraulic actuators offer several advantages over their electrical counterparts. Hydraulics actuators are light-weight and offer large force/torque output. They are inert to fire hazards and are widely available in mobile applications. On the other hand, hydraulics introduce additional non-linearities to the control problem. In contrast to electrical actuators, the current input to the hydraulic actuator modulates the valve opening instead of the torque output of the actuator. Therefore, in order to design a controller that achieves robust interaction between a hydraulic manipulator and its environment, a model-based approach is pursued [4], [9]. A dynamic model of the robot's joint used in this research was derived in a previous research paper [1].

The control of manipulators interacting with their environment has received considerable attention, mostly dealing with electrically actuated manipulators. Two main controller designs have been developed, hybrid position/force control, [14], and impedance control, [6]. In hybrid position/force control, the task space is divided into two subspaces. Forces are controlled in the constrained directions while positions are controlled in the unconstrained directions. Control law switching is required for transition from free space to contact with an environment [2], [3]. In addition, the environment location and geometry is required. On the other hand, the goal of the impedance control scheme is to control the manipulator-environment interaction rather than individual forces or positions. No control law switching is required, since the same controller can be used for both contact and noncontact tasks. Impedance control is inherently a model-based approach. Two approaches exist, namely, position-based impedance control and torque-based impedance control. The two have been discussed in [8]. In the position-based approach, positions are commanded while forces are measured. An impedance filter modifies the position command, therefore, it relies on an existing or specially designed position controller other than the manufacturer's controller, [5], [8], [13], [15]. This approach can readily be used for position-controlled manipulators including hydraulically actuated ones. In the torque-based (classical) approach, positions and forces are measured while torques

0-7803-4465-0/98 $10.00 © 1998 IEEE

are commanded. [6]. The latter is suitable for electrical actuators since motor torque is proportional to the input current.

In this paper, position-based impedance control of a hydraulic servo-actuator joint is studied. The goal here is first to impart a desired behavior to the hydraulically-actuated SARCOS manipulator elbow joint, and then to the entire manipulator. To deal with system physics and complexity, a feedforward, model-based block has been introduced to an impedance control scheme. Although feedforward control has been used previously in tracking tasks of a hydraulic flexible manipulator, it has not been employed before in the case of hydraulic manipulators interacting with an environment [7]. The model-based feedforward part of the controller is derived here from a detailed system model obtained previously [1]. In the case of free-space motion, step response results demonstrate the attainment of desired behavior. In the case of contact, proper choice of impedance and control parameters results in smooth contact transition and desired force application. The paper is structured as follows. In Section 2, the hydraulic system is described. Section 3 discusses briefly the theory of impedance control and some of its extensions. An impedance controller for the hydraulic actuator is designed in Section 4. Implementation results are shown in Section 5 for the case of step inputs, trajectory following and contact cases. Finally, Section 6 closes with some conclusions.

2 Hydraulic Actuator and Model Description

The hydraulic system used in this study is briefly described in this section. In addition, a reduced order model is derived for control purposes. Notation used throughout the paper is shown in Table 1.

2.1 System Description

The system studied is the elbow joint of the SARCOS hydraulic slave manipulator. A schematic diagram of the system is illustrated in Figure 1.

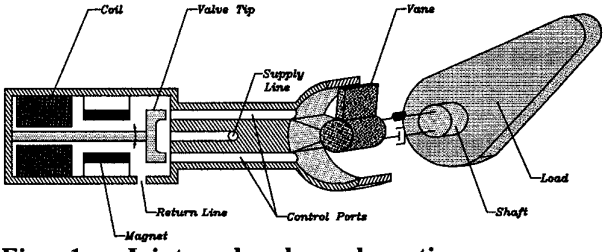

Fig. 1. Joint and valve schematic.

Several key systems are shown: the servovalve, the vane actuator and the load. The servovalve is of a jet-pipe/suspension type design. Input current modulates the valve tip motion, which adjusts flow into the vane actuator through the two control ports. Vane and load motion results. Detailed modeling of this system is described in [1]. This model consists of twelve first order nonlinear differential equations. Some highly nonlinear physical phenomena were modeled including servovalve hysteresis, nonlinear flow-pressure orifice relationships, orifice geometry, and viscous and Coulomb friction. Valve tip dynamics were identified as a second-order system excited by the input current and flow forces at the valve tip. Fluid dynamics are characterized considering line losses, turbulent flow through the orifices, leakage due to gaps between the valve tip and receiver, and oil compressibility, [11]. A more detailed presentation of the model as well as the associated parameter identification experiments and results are found in [1]. The model, in its detailed form, is useful in understanding the physical phenomena in the system and can be used to evaluate controller performance in simulation. However, for control design, a reduced order model is needed to reduce computational effort. Thus, the reduced order model is discussed in the next section.

Table 1. Nomenclature.

Variable	Definition
i, i_{ff}, i_{fb}	total, feedforward, and feedback current.
B	servovalve motor torque constant
x_v, A_i	valve tip displacement, i-th orifice area
ζ_n, ω_n	damping ratio and natural frequency of valve tip dynamics.
V_{c1}, P_{p1}	volume and pressure in chamber 1.
V_{c2}, P_{p2}	volume and pressure in chamber 2.
V_{p1}, V_{p2}, V_t	volume of line of ports 1 and 2, total volume
ρ, μ, β	density, viscosity and bulk modulus of oil.
P_l, Q_l	load pressure and load flowrate.
P_s, P_{lr}	supply and return pressure.
C_d	discharge coefficient.
R_v	leakage coefficient of rotary actuator.
D_v	rotary actuator volumetric displacement.
W_l	weight of load.
J_l	lumped load, shaft and vane rotary inertia.
b_l	lumped load, shaft and vane damping.
M_d, B_d, K_d	impedance parameters: inertia, damping and stiffness.
B_f, K_f	impedance parameters: coefficients of torque rate and torque.
K_e	environment torsional stiffness.
ω_{vn}	vane angular velocity.
θ, θ_d	angular position of load and desired position.
τ_e, τ_{act}	external torque and actuator torque.
τ_c	desired contact torque.
K_p, K_v, K_{pl}	feedback gains.

2.2 System Model for Control

To achieve maximum trajectory tracking accuracy and minimum control effort, with reasonable computational cost, the dominant dynamics of the system need to be retained from the detailed model. For this, some simplifying assumptions are required. Since the natural frequency of the servovalve is quite high compared to other system dynamics, it is reasonable to assume that, at least, for control system design purposes the second order dynamics can be reduced such that the valve tip position is proportional to the input current,

$$x_v = \frac{B}{\omega_n^2} i \qquad (1)$$

At the level of flow dynamics, it is assumed that leakage from supply to return can be neglected, that is, there is no clearance between the valve tip and its receiver. The flow dynamics most significant for control purposes are those present in the actuator. The differential equations describing the chamber pressures are [1],

$$\dot{P}_{p1} = \frac{\beta}{(V_{c1}+V_{p1})}\Big(g_1(x_v,P_S,P_{p1}) - g_4(x_v,P_{p1},P_{rl}) - D_v\omega_{vn} - R_v(P_{p1}-P_{p2})\Big) \quad (2)$$

$$\dot{P}_{p_2} = \frac{\beta}{\left(V_{c_2}+V_{p_2}\right)}\Big(g_2\left(x_v,P_S,P_{p_2}\right) - g_3\left(x_v,P_{p_2},P_{rl}\right) + D_v\omega_{vn} + R_v\left(P_{p_1}-P_{p_2}\right)\Big) \quad (3)$$

where,

$$g_i(x_v,P_{hi},P_{lo}) = C_d A_i(x_v)\sqrt{(P_{hi}-P_{lo})\cdot 2/\rho}, \quad i=1,\ldots 4 \quad (4)$$

Subtracting the two chamber pressure equations, Eq. (3) from Eq. (2), yields

$$(V_{c1}+V_{p1})\dot{P}_{p1} - (V_{c2}+V_{p2})\dot{P}_{p2} = \beta\Big((g_1-g_2)-(g_4-g_3) - 2D_v\omega_{vn} - 2R_v(P_{p1}-P_{p2})\Big) \quad (5)$$

which can be rewritten as,

$$\big(V_c+f(\theta)\big)\dot{P}_{p1} - \big(V_c-f(\theta)\big)\dot{P}_{p2} = \beta\Big((g_1-g_2)-(g_4-g_3) - 2D_v\omega_{vn} - 2R_v(P_{p1}-P_{p2})\Big) \quad (6)$$

Here, V_c is the chamber volume when $\theta = 0$ and $f(\theta)$ is the volume of the fluid displaced as a function of the angular position of the vane. Assuming that the valve can be described as an ideal critical center valve with matched and symmetrical orifices the load flow and chamber pressures can be determined as [11],

$$g_1 - g_4 = g_3 - g_4 = Q_L$$
$$Q_L = C_d w_x x_v \sqrt{P_S - \frac{x_v}{|x_v|}P_L}$$
$$P_{p1} = \frac{P_S+P_L}{2}, P_{p2} = \frac{P_S-P_L}{2} \quad (7)$$

from which a reasonable assumption follows,

$$\dot{P}_{p1} + \dot{P}_{p2} \cong 0 \quad (8)$$

Using Eqs. (7) and (8), Eq. (6) is simplified, and can be rewritten in a more familiar form in terms of the load pressure and the load flow [11],

$$Q_l = \frac{V_t}{4\beta}\dot{P}_l + D_v\omega_{vn} + R_v P_l \quad (9)$$

In reducing the vane and load system equations, the friction and shaft flexibility are neglected. Thus, the dynamics of the vane and load can be expressed as,

$$J_l\ddot{\theta} + b_l\dot{\theta} + W_l\sin\theta = \tau_{act} = D_v P_l \quad (10)$$

Eqs. (9) and (10) define the reduced order model, which is used in the controller development, while the detailed model in [1] is taken as the truth system model to be controlled. The saturation of the current input was also modeled since the physical system's input current can take on values between +/- 1 amp.

3 Position-Based Impedance Control

Impedance control essentially allows a physical system to emulate another more simple system assuming the new behavior is within the capabilities of the physical system. In the following, a short introduction to position-based impedance control and its implementation is given.

3.1 Implementation Example

In the position-based impedance approach, a new trajectory is computed using an impedance filter. This new trajectory reflects the desired behavior based on the impedance parameters and the measured contact force. It serves as the new command to an inner position control loop. The control system is shown in Figure 2.

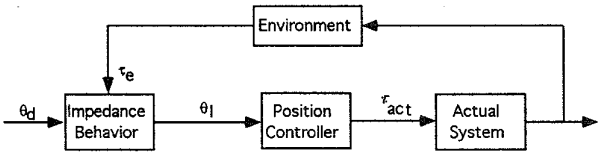

Fig. 2. Schematic of Position-based Impedance Control.

Consider impedance control of an actuated mass interacting with an environment. The system equation is given as,

$$M\ddot{\theta} = \tau_{act} + \tau_e \quad (11)$$

where M denotes the inertia of the system and the contact torque is given by τ_e which can be measured using a torque sensor. For simulation purposes, it may also be estimated, assuming a stiff environment, as

$$\tau_e = K_e(\theta_e - \theta) \quad (12)$$

A typical system behavior is given by second order dynamics, such that [6]

$$M_d\ddot{\theta} + B_d\dot{\theta} + K_d(\theta-\theta_d) = \tau_e \quad (13)$$

where M_d, B_d, and K_d are impedance parameters describing the desired second order behavior. Let θ_l denote the new position command, as shown in Figure 2. It may be found from,

$$M_d\ddot{\theta}_l + B_d\dot{\theta}_l + K_d\theta_l = \tau_e + K_d\theta_d \quad (14)$$

The new trajectory, θ_l, depends on the desired one, θ_d, and on the contact torque. In the case of free space, the contact force is zero. Here, the impedance filter modifies the desired trajectory according to the parameters, M_d, B_d, and K_d. In the case of contact, θ_d, is known as a virtual position which is not attained but is helpful in regulating the force applied to an environment if environment location and properties are well known *a priori*. This is accomplished by specifying some position within the environment.

The desired behavior can be extended to include the error in velocity, acceleration and in general, the force. This formulation is termed the generalized impedance, [10]. The desired impedance is given as,

$$M_d(\ddot{\theta}-\ddot{\theta}_d)+B_d(\dot{\theta}-\dot{\theta}_d)+K_d(\theta-\theta_d) = B_f(\dot{\tau}_e+\dot{\tau}_c)+K_f(\tau_e+\tau_c) \quad (15)$$

Here, both a desired position trajectory and a contact torque trajectory is specified by the user along with the impedance parameters. This formulation is useful if the environment properties are uncertain [10].

3.2 Impedance Parameter Selection

Correct parameter selection allows a desired behavior to be attained while providing favorable response. For example, in most tasks involving contacts, it is desirable that the transition from free space to contact be accomplished without oscillations. The characteristic equation for the case of contact can be found from Eq. (15) to be,

$$F(s) = M_d s^2 + \left(B_d + B_f K_e\right)s + \left(K_d + K_f K_e\right) \quad (16)$$

As shown by Eq. (16), the environment stiffens the combined manipulator-environment system. Assuming constant desired torque and a stationary environment, the requirement for no oscillations dictates a critically damped or an overdamped second-order system. This gives,

$$\left(B_d + B_f K_e\right)^2 \geq 4M_d\left(K_d + K_f K_e\right) \quad (17)$$

Which may be expanded to,

$$B_f^2 K_e^2 + \left(2B_d B_f - 4M_d K_f\right)K_e + \left(B_d^2 - 4M_d K_d\right) \geq 0 \quad (18)$$

In the simulations of Section 5, Eq. (18) provides a guideline for stable contact. For B_f = 0 and K_f = 1, increasing B_d such that Eq. (18) is satisfied, allows good performance in the presence of an environment. One may also reduce the desired mass or the desired stiffness, keeping desired damping constant. However, there are physical limitations to be respected, since the choice of impedance parameters affects the control input. A desired behavior may require the system to go beyond its physical capacity thus limiting the attainable impedance. In addition, unmodeled dynamics may be excited due to impedance parameter choices. For the highly nonlinear hydraulic system, a model-based impedance control allows dominant dynamics to be accounted for while providing good impedance behavior. Hence, by studying the linearized control system in the Laplace domain, impedance parameters are selected to give non-oscillatory response. These parameters are fine-tuned in the control of the nonlinear system. The next section discusses the design of the impedance controller.

4 Feedforward Impedance Control Design

Given a desired system behavior to be emulated, a suitable feedforward input current must be determined such that the physical system behaves like the desired system in noncontact and contact regimes. In the case of the hydraulic joint, one must consider both the dynamics of the hydraulic and mechanical subsystems. Schematically, the proposed control scheme is shown in Figure 3. As shown in this figure, the commanded trajectory is modified by the *Impedance Behavior* block, whose output, θ_l, depends on feedback of the interaction forces/torques with the environment. In more detail, the impedance trajectory output, θ_l, is determined from

$$M_d\ddot{\theta}_l + B_d\dot{\theta}_l + K_d\theta_l = M_d\ddot{\theta}_d + B_d\dot{\theta}_d + K_d\theta_d + B_f\left(\dot{\tau}_e+\dot{\tau}_c\right)+K_f\left(\tau_e+\tau_c\right) \quad (19)$$

This trajectory is fed into a feedforward block which implements the simplified model of the joint, described by Eqs. (9) and (10). Thus, Eq. (10) results in

$$J_l\ddot{\theta}_l + b_l\dot{\theta}_l = D_v P_l - W_l\sin\theta_l + \tau_e \quad (20)$$

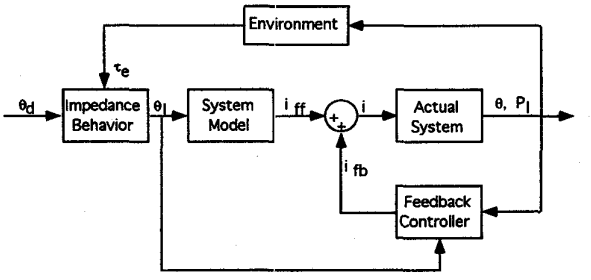

Fig. 3. Control System Scheme.

The load pressure P_l, that corresponds to the impedance trajectory, θ_l, is given by

$$P_{ll} = \frac{1}{D_v}\left(J_l\ddot{\theta}_l + b_l\dot{\theta}_l + W_l\sin\theta_l - \tau_e\right) \quad (21)$$

Direct substitution of the load pressure P_l, and its derivative, and substitution of the angular velocity ω_{vn} by θ_l, into the hydraulics dynamics given by Eq. (9), yields the feedforward component of the current,

$$i_{ff} = \frac{1}{K\sqrt{P_s - P_{ll}}}\left[\frac{V_t}{4\beta}\dot{P}_{ll} + R_v P_{ll} + D_v\dot{\theta}_l\right] \quad (22)$$

The feedforward current may be computed on-line or off-line. In the case of contact, the computation will need to be done on-line unless a good model of the environment exists.

In addition to the feedforward loop, a feedback loop is implemented to compensate for discrepancies between the actual system and the feedforward model. This loop can be composed of a variety of terms depending on robustness and performance required. Examples include the following feedback laws,

$$i_{fb} = K_p\left(\theta-\theta_l\right)+K_v\left(\dot{\theta}-\dot{\theta}_l\right)$$
$$i_{fb} = K_p\left(\theta-\theta_l\right)+K_v\left(\dot{\theta}-\dot{\theta}_l\right)+K_{Pl}\left(P_l-P_{ll}\right) \quad (23)$$

The latter, which is used here, increases the bandwidth with respect to the previous feedback controller. Position, velocity and load pressure are required for feedback. Control may also be based on sliding mode and adaptive schemes.

5 Simulation Results

The controller developed in the previous section is implemented here using as plant the detailed system in order to evaluate its performance. The simulations were run in

MATLAB using the Gear integration method. First, through step responses, it is shown that the hydraulic joint response emulates a desired behavior. Next, the controller's ability to track a trajectory with respect to a prescribed behavior is demonstrated in free space as well as in contact.

5.1 Step Response

The elbow, whose schematic is shown in Figure 1, is commanded by a step setpoint of 0.4 radians with a desired behavior specified by a target natural frequency of 10 rad/s and damping ratios of 0.6, 1.0 and 1.6. The impedance parameters, B_f and K_f are set to zero since the motion is strictly in free space. The impedance parameters are chosen so that valve current saturation is avoided. Feedback parameters are chosen such that good response is obtained and that the unmodeled dynamics such as those due to the servovalve and the hydraulic lines are well compensated for. The feedback gains have the following values,

$$K_p = 7.0,\ K_v = 0.20,\ K_{pl} = 0.001$$

Beyond these values, either no change was observed in the response or the response showed undesirable oscillations. The results are shown in Figure 4. The error between the actual response and the impedance trajectory were low, on the order of 0.012 radians. In the steady state, the error drops to 0.006 radians and may be due to unmodeled leakage. Further tuning of the feedback gains would reduce this error. The response of the error over time is shown in Figure 5.

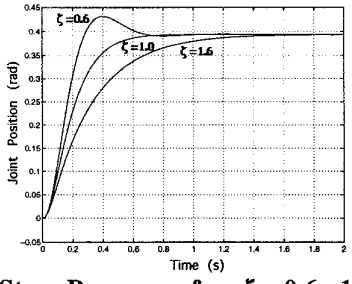

Fig. 4. Step Response for ζ_d=0.6, 1.0, & 1.6.

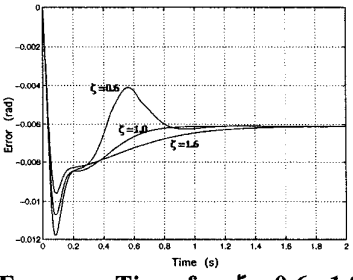

Fig. 5. Error vs Time for ζ_d=0.6, 1.0 and 1.6.

Next, consider the control current which is composed of a feedforward and a feedback component, see Fig. 6. This figure illustrates only the current input for the overdamped case (ζ = 1.6). As shown in Fig. 6, the feedforward current indicates that the reduced order model captures well the dynamics of the mechanical and hydraulic subsystems. The feedback current introduces an active control effort as reflected by the high frequency decaying oscillations. In the end, the control system imparts the desired behavior to the hydraulic joint with a small feedback effort.

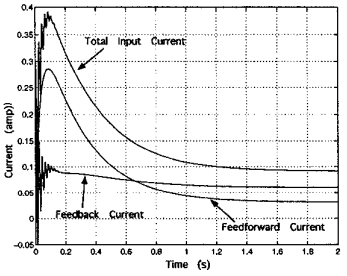

Fig. 6. Current Inputs for ζ_d=1.6.

5.2 Free Space and Contact

In the following, a cycloidal trajectory was commanded to the elbow of Figure 1. A cycloidal trajectory is chosen for its practicality and future use in experimental work. Here, the initial conditions for joint position, velocity and acceleration are all zero. The trajectory has a duration of 1 second and attains a maximum of 0.3 radians. An environment of torsional stiffness, K_e = 1000 lb-in/rad (113 Nm/rad), is placed at 0.1 radians. Zero desired contact torque is specified when contact is made. The desired trajectory and environment location are shown in Figure 7.

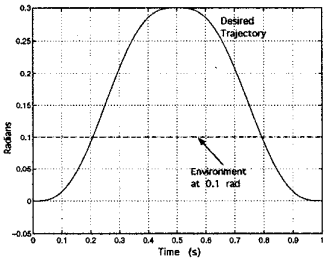

Fig. 7. Desired Trajectory and Environment Location.

Impedance parameters were selected according to Eq. (18), such that,

$$M_d = 1,\ K_d = 4900,\ B_d = 700,\ K_f = 50$$

The impedance parameter, B_f, was set to zero to avoid use of second time derivatives of the contact torque in the *Impedance Behavior* block, see Fig. 3. Use of such derivatives is not practical as it would introduce undesired noise and input current saturation, especially during contact. The feedback gains were taken to be,

$$K_p = 7,\ K_v = 0.2,\ K_{pl} = 0.0003$$

The response of the hydraulic system, shown in Figure 8, follows closely the desired one. Upon contact, no oscillations are observed and a desired behavior is obtained. In the case of an impact, the load pressure rate can be high and the servovalve dynamics may be excited unless proper compensation is present. The choice of the feedback gain on load pressure of K_{pl} = 0.0003 eliminated the oscillations.

Figure 9 illustrates the development of a contact torque of just over 2.5 Nm on the environment. The desired contact torque was set at zero. The controller is successful in producing a smooth transition to contact with the environment. Input current is depicted in Figure 10. In free space, feedforward current is larger than the feedback control effort indicating, again, that the reduced model reflects well the dynamics of the actual system. However, at contact, as the control system attempts to follow the desired behavior, the feedback current increases in activity reflected by the oscillations just after 0.2 seconds. Thus, the importance of good feedback compensation during transition is demonstrated.

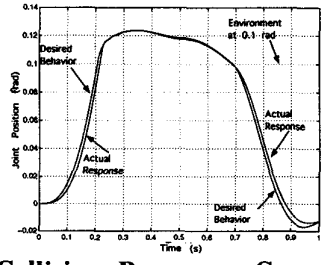

Fig. 8. Collision Response: Comparison to Desired Behavior.

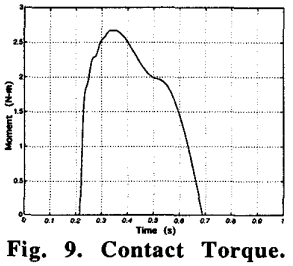

Fig. 9. Contact Torque.

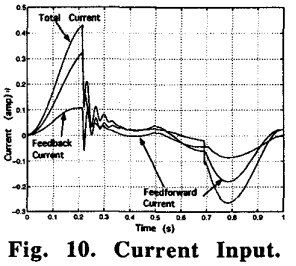

Fig. 10. Current Input.

7 Conclusions

A model-based, feedforward-feedback impedance controller was developed for a high-performance hydraulic joint, using a position-based impedance scheme. An impedance filter adjusts the desired trajectory according to a prescribed behavior in free space and in contact. The model-based portion of the controller implements a reduced order model of the system and computes a feedforward current accounting for the dominant dynamics and reducing the feedback control effort. Simulation results using step responses indicated that the controller was successful in achieving a desired behavior. The model-based portion significantly reduced the feedback control effort. Furthermore, the controller worked well in free space and in contact. In all, results showed that the developed impedance control scheme is promising for hydraulic servoactuated joints. It is expected that ongoing work in parameter tuning and practical implementation, e.g. feedforward evaluation of the model, will further improve the system's performance.

8 Acknowledgments

The support of this work by the Fonds pour la Formation de Chercheurs et l'Aide à la Recherche (FCAR), and by the Natural Sciences and Engineering Council of Canada (NSERC) is gratefully acknowledged.

References

[1] Bilodeau, G. and Papadopoulos, E., "Modelling, Identification and Experimental Validation of a Hydraulic Manipulator Joint for Control," *IEEE/RSJ Int. Conf. on Intell. Robots and Sys.*, pp. 331-336, 1997.

[2] Bluethmann, B., et. al., "Experiments in Dexterous Hybrid Force & Position Control of a Master/ Slave Electrohydraulic Manipulator," *IEEE/RSJ Int. Conf. on Intell. Robots and Sys.*, Vol. 3, pp. 27-32, 1995.

[3] Dunnigan, M.W., et. al., "Hybrid Position/Force Control of a Hydraulic Underwater Manipulator," *IEE Proc.: Control Theory and Applications*, Vol. 143, No. 2, pp. 145-151, March 1996.

[4] Egeland, O., "Cartesian Control of a Hydraulic Redundant Manipulator," *IEEE Int. Conf. on Robot. and Autom.*, pp. 2081-2087, 1987.

[5] Heinrichs, B., Sepehri, N., and Thornton-Trump, A.B., "Position-Based Impedance Control of an Industrial Hydraulic Manipulator," *IEEE Int. Conf. on Robot. and Autom.*, pp. 284-290, 1996.

[6] Hogan, N., "Impedance Control: An approach to manipulation: Part I - Theory, Part II - Implementation, part III - Applications", *ASME Journal of Dynamic Systems, Measurement, and Control*, Vol. 107, pp. 1-24, March 1985.

[7] Kwon, D.S., et. al., "Tracking Control of the Hydraulically Actuated Flexible Manipulator," *IEEE Int. Conf. on Robot. and Autom.*, pp. 2200-2205, 1995.

[8] Lawrence, D.A., "Impedance Control Stability Properties in Common Implementations," *IEEE Int. Conf. on Robot. and Autom.*, pp. 1185-1190, 1988.

[9] Leahy, M.B., and Saridis, G.N., "Compensation of Industrial Manipulator Dynamics," *The Int. J. of Robotics Research*, Vol. 8, No. 4, pp.73-84, 1989.

[10] Lee, S., and Lee, H.S., "Intelligent Control of Manipulators Interacting with an Uncertain Environment Based on Generalized Impedance," *Proc. IEEE Int. Symp. on Intell. Control*, pp.61-66, Aug. 1991.

[11] Merritt, H.E., Hydraulic Control Systems, New York: John Wiley and Sons Inc., 1967.

[12] Papadopoulos, E., et. al., "On the Modeling and Control of an Experimental Harvester Machine Manipulator," *IEEE/RSJ Int. Conf. on Intell. Robots and Sys.*, pp. 1832-1837, 1997.

[13] Pelletier, M., and Doyon, M., "On the Implementation and Performance of Impedance Control on Position Controlled Robot," *IEEE Int. Conf. on Robot. and Autom.*, pp. 1228-1233, 1994.

[14] Raibert, M.H., and Craig, J.J., "Hybrid position/force control of manipulators," *ASME Journal of Dynamic Systems, Measurement and Control*, Vol. 102, pp. 126-133, June 1981.

[15] Seraji, H., and Colbough, R., "Force Tracking in Impedance Control," *The Int. Journal of Robotics Research*, Vol. 16, No. 1, pp.97-117, 1997.